# Cross-hemispheric dopamine projections have functional significance

Megan E. Fox[a,b], Maria A. Mikhailova[c], Caroline E. Bass[d], Pavel Takmakov[a,b,1], Raul R. Gainetdinov[c], Evgeny A. Budygin[c,e], and R. Mark Wightman[a,b,2]

[a]Department of Chemistry, University of North Carolina at Chapel Hill, Chapel Hill, NC 27599; [b]UNC Neuroscience Center, UNC School of Medicine, University of North Carolina at Chapel Hill, Chapel Hill, NC 27599; [c]Institute of Translational Biomedicine, St. Petersburg State University, St. Petersburg 199034, Russia; [d]Department of Pharmacology and Toxicology, Jacobs School of Medicine and Biomedical Sciences, University at Buffalo, Buffalo, NY 14260; and [e]Department of Neurobiology and Anatomy, Wake Forest School of Medicine, Winston Salem, NC 27157

Edited by Richard D. Palmiter, University of Washington, Seattle, WA, and approved May 12, 2016 (received for review March 3, 2016)

**Dopamine signaling occurs on a subsecond timescale, and its dysregulation is implicated in pathologies ranging from drug addiction to Parkinson's disease. Anatomic evidence suggests that some dopamine neurons have cross-hemispheric projections, but the significance of these projections is unknown. Here we report unprecedented interhemispheric communication in the midbrain dopamine system of awake and anesthetized rats. In the anesthetized rats, optogenetic and electrical stimulation of dopamine cells elicited physiologically relevant dopamine release in the contralateral striatum. Contralateral release differed between the dorsal and ventral striatum owing to differential regulation by D2-like receptors. In the freely moving animals, simultaneous bilateral measurements revealed that dopamine release synchronizes between hemispheres and intact, contralateral projections can release dopamine in the midbrain of 6-hydroxydopamine–lesioned rats. These experiments are the first, to our knowledge, to show cross-hemispheric synchronicity in dopamine signaling and support a functional role for contralateral projections. In addition, our data reveal that psychostimulants, such as amphetamine, promote the coupling of dopamine transients between hemispheres.**

dopamine | voltammetry | synchrony | nucleus accumbens | dorsal striatum

Dopamine neurotransmission modulates arousal and motivation, and is important to the expression of reward-seeking behavior. Dopamine is released on a subsecond timescale during unexpected reward (1, 2), and becomes time-locked to cues that predict reward (3–7). Dopamine transients in the nucleus accumbens (NAc) occur as a result of cell firing in the ventral tegmental area (VTA) (8, 9), and in rats reach concentrations of 50–200 nM before returning to baseline (10, 11). Striatal dopamine transients also occur spontaneously during periods of rest (10, 11), reflecting endogenous dopamine modulation. The magnitude and frequency of dopamine transients increase in response to drugs of abuse (12, 13), which is thought to contribute to their reinforcing properties (14). Although numerous studies have summarized the function of dopamine circuits in reward-based behaviors (15, 16) and motor control (17–19), anatomic descriptions of dopamine projections are conflicting (20–23). Recent evidence suggests that some dopamine neurons project contralateral to their origin (22, 23), contradictory to the uncrossed dopamine system described previously (20, 21). To date, the significance of contralaterally projecting dopamine neurons, and how they may contribute to cross-hemispheric signaling, have not been established.

A potential role for contralateral dopamine projections emerged in a recent study on brain stimulation reward (24). When rats were trained to self-stimulate the VTA, infusion of dopamine receptor antagonists in the NAc suppressed stimulation. This effect was seen whether the infusion was contralateral or ipsilateral to the stimulation site, reflecting cross-hemispheric modulation of the behavior. Furthermore, c-Fos, a marker of neural activity, was elevated in both hemispheres after unilateral stimulation. Because the study did not examine dopamine release from VTA stimulation, the functional influence of contralateral projections could not be confirmed.

Contralateral projections also may play a role in the neural adaptations in Parkinson's disease, which is characterized by a loss of midbrain dopamine. A hemiparkinsonian state can be modeled with unilateral 6-hydroxydopamine (6-OHDA) lesions, and recent studies have described alterations in synaptic signaling following dopamine depletion (25–29). If contralateral dopamine projections have functional significance, then dopamine arising from these intact projections may influence signaling in the lesioned hemisphere (30). Understanding the influence of contralateral projections may afford new approaches to implementing such therapies as deep brain stimulation for Parkinson's disease.

In this study, we demonstrate that contralaterally projecting dopamine neurons are functional and influence cross-hemispheric striatal signaling. We measured spontaneous and stimulated dopamine release in rats with fast-scan cyclic voltammetry (FSCV). In freely moving rats, we found spontaneous synchronous dopamine release in both hemispheres that further synchronized following amphetamine administration. We show that electrical or optogenetic stimulation of dopamine neurons elicits physiologically relevant dopamine release in the contralateral NAc and dorsomedial striatum (DMS). Using pharmacology, we show that dopamine projections are differentially regulated by D2 receptors.

## Significance

**Decades of research have described dopamine's importance in reward-seeking behavior and motor control. Although numerous investigations have focused on dopamine's mechanisms in modulating behavior, the long-standing belief that dopamine neurons project solely unilaterally has limited the exploration of interhemispheric dopamine signaling. Here we resolve disparate descriptions of unilateral vs. bilateral projections by reporting that dopamine neurons can release dopamine in the contralateral hemisphere. Using voltammetry in awake and anesthetized rats, we reveal an unprecedented synchrony of dopamine fluctuations between hemispheres. Via stimulation with amphetamine, we demonstrate functional cross-hemispheric projections in a hemiparkinsonian model. This previously undescribed capacity for interhemispheric dopamine signaling can precipitate new areas of inquiry. Future work may exploit properties of bilateral dopamine release to improve treatments for Parkinson's disease, including deep brain stimulation.**

Author contributions: P.T. performed the initial bilateral pilot experiments in anesthetized rats that inspired the study; M.E.F., E.A.B., and R.M.W. designed research; M.E.F., M.A.M., C.E.B., P.T., and E.A.B. performed research; C.E.B. contributed new reagents/analytic tools; M.E.F., M.A.M., C.E.B., and E.A.B. analyzed data; and M.E.F., R.R.G., E.A.B., and R.M.W. wrote the paper.

The authors declare no conflict of interest.

This article is a PNAS Direct Submission.

[1]Present address: Division of Biology, Chemistry, and Material Sciences, Office of Science and Engineering Laboratories, Center for Devices and Radiological Health, US Food and Drug Administration, White Oak Federal Research Center, Silver Spring, MD 20993.

[2]To whom correspondence should be addressed. Email: rmw@unc.edu.

This article contains supporting information online at www.pnas.org/lookup/suppl/doi:10.1073/pnas.1603629113/-/DCSupplemental.

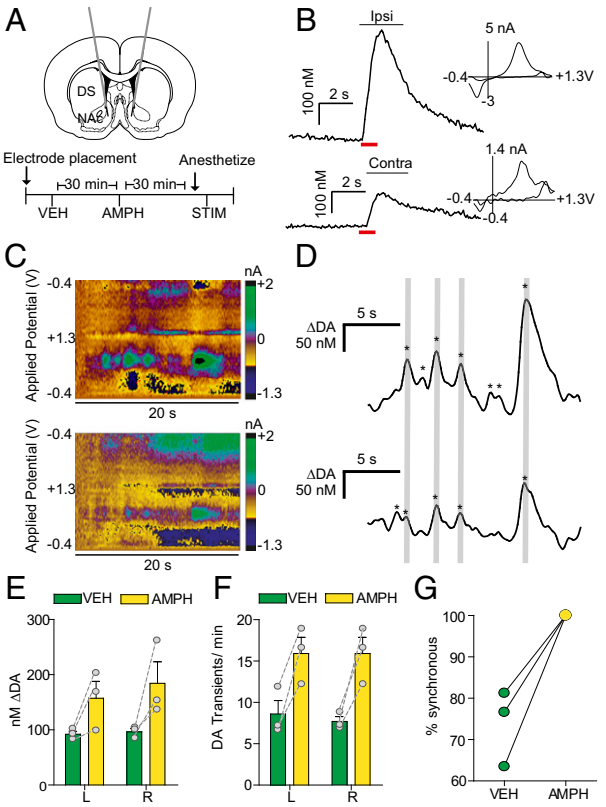


**Fig. 1.** Spontaneous dopamine transients synchronize bilaterally in the NAc. (*A*) Schematic of electrode implantation for simultaneous dopamine transient measurements. (*B*) Representative dopamine release in the right and left NAc following stimulation (red bar) of the right VTA, with voltammograms. (*C*) Representative color plots demonstrating synchronous dopamine transients in both hemispheres with applied potential on the ordinate, recording time on the abscissa, and current encoded in false color. (*D*) Changes in dopamine concentration (asterisks) in both hemispheres extracted using principal component analysis from the color plots in *C*. Gray lines indicate synchronized transients; asterisks alone indicate asynchronous dopamine release. (*E*) Average ± SEM dopamine transient concentration in the left (L) and right (R) NAc after administration of saline vehicle (VEH; green) and 2.5 mg/kg amphetamine (AMPH; yellow). (*F*) Average ± SEM number of dopamine transients $min^{-1}$ in the left and right NAc after VEH and AMPH administration. (*G*) Within-animal comparison of percent transient synchrony after VEH and AMPH administration. $n = 3$ animals.

We also extend these findings into 6-OHDA–lesioned animals and characterize functional adaptations following unilateral depletion.

## Results

**Spontaneous Dopamine Transients Synchronize in the NAc.** FSCV has been used to measure dopamine fluctuations in a number of studies; however, to date, all awake-animal measurements have been restricted to a single hemisphere (1–13, 31–35). To investigate connectivity between hemispheres, we measured dopamine transients bilaterally in the NAc of freely moving rats. We recorded from dual carbon fiber electrodes, as used previously in anesthetized animals (36). We targeted guide cannulas over the NAc (Fig. 1*A*) and optimized recording locations for spontaneous dopamine release (Fig. 1 *C* and *D*). We found dopamine transients of similar magnitudes (left, 92.1 ± 5.23 nM; right, 96.4 ± 5.92 nM; Fig. 1*E*) and frequency (left, 8.5 ± 1.6 transients $min^{-1}$; right, 7.7 ± 0.6 transients $min^{-1}$; Fig. 1*F*) in both hemispheres. Interestingly, 74 ± 5.3% of dopamine transients occurred simultaneously between hemispheres in animals at rest (Fig. 1*G*). We next administered d-amphetamine (AMPH; 2.5 mg/kg i.p.), and found that transient magnitude increased in both hemispheres (left, 157.2 ± 30.6 nM; right, 184.3 ± 39.2 nM, two-way repeated-measures ANOVA; effect of AMPH, $F_{(1,4)} = 11.3$, $P < 0.05$) (Fig. 1*E*). Following AMPH administration, all dopamine transients synchronized and increased in frequency (15.9 ± 2.0 transients $min^{-1}$, two-way repeated-measures ANOVA; effect of AMPH, $F_{(1,4)}=13.7$, $P < 0.05$) (Fig. 1 *F* and *G*). With animals anesthetized and the VTA stimulated unilaterally, we measured dopamine at both electrodes (Fig. 1*B*).

**Stimulation of Dopamine Neurons Elicits Release in the Contralateral Hemisphere.** Given that electrical stimulation of the VTA resulted in dopamine in both hemispheres, we characterized contralaterally evoked release to ascertain whether it was restricted to the NAc, and whether it contributed to coupled dopamine transients. We implanted a carbon fiber electrode into either the NAc or DMS (Fig. 2 *A* and *D*) of anesthetized rats and lowered it ventrally through the striatum with the stimulating electrode in the contralateral VTA [8.8 mm dorsoventral (DV)] or substantia nigra (SN; 7.6 mm DV). We found multiple locations that supported release (Fig. 2 *B* and *E*). In the NAc, contralateral dopamine release peaked ($DA_{con}/DA_{con\text{-}max}$) in the core (6.4 mm DV) and in the shell (7.4 mm DV; Fig. 2*C*). In the DMS, maximal dopamine release elicited by contralateral SN stimulation was restricted to a smaller range (6.2–6.4 mm DV; Fig. 2*F*).

We examined interhemispheric differences using within-animal comparisons of dopamine evoked contralateral vs. ipsilateral to the stimulation site (Fig. 3 *A* and *C*). With the recording electrode at a constant depth (NAc, 7.4 mm DV; DMS, 6.2 mm DV), maximal release was achieved by stimulating similar VTA or SN depths in both hemispheres. Of note, in the NAc, ipsilateral stimulation elicited ∼20-fold more dopamine release than contralateral stimulation (8.8 mm DV; Fig. 3*A*). In contrast, ipsilateral and contralateral SN stimulations evoked dopamine release of equal magnitude in the DMS (7.6 mm DV; Fig. 3*C*). We obtained similar release in the DMS by stimulating the contralateral and ipsilateral peduncolopontine tegmental nucleus (PPTg), an excitatory input to the SN (Fig. S1). Recording in the dorsolateral striatum revealed that

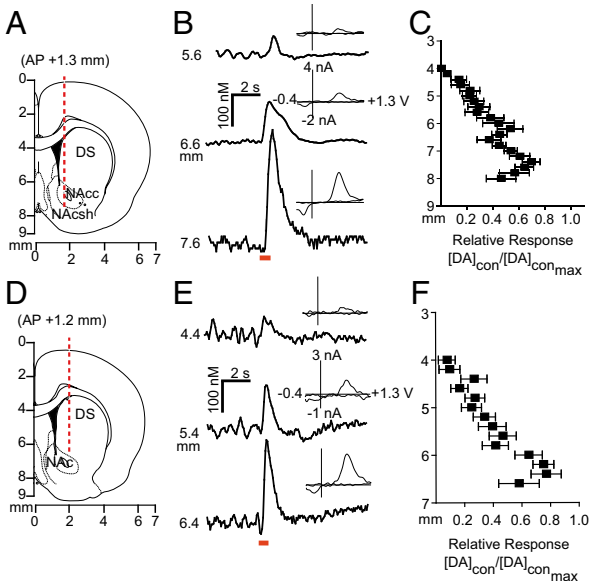


**Fig. 2.** Stimulation of dopamine neurons produces localized release in the contralateral striatum. (*A* and *D*) Electrode trajectories superimposed on coronal sections. (*B* and *E*) Dopamine release at the terminals was dependent on recording electrode depth; example traces are shown. Cyclic voltammograms recorded at maximum release are shown as well. (*C* and *F*) Dopamine response ($DA_{con}$) following electrical stimulation of the contralateral VTA (*C*) or SN (*F*), normalized to maximum dopamine release ($DA_{con\text{-}max}$) as a function of working electrode depth. $n = 10$ animals per group. Data are average ± SEM.

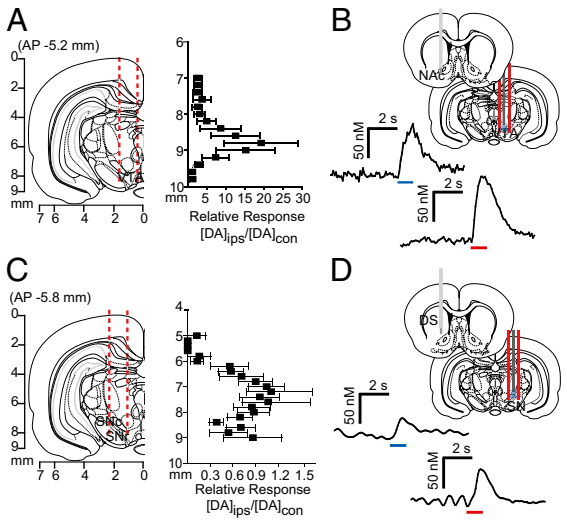


**Fig. 3.** Stimulation of contralateral dopamine neurons produces variable dopamine release in the striatum. (*A* and *C*) Coronal sections showing stimulating electrode tracts in the VTA (*A*) and SN (*C*), and within-animal comparison of NAc and DMS effluxes, resulting from ipsilateral stimulation ($DA_{ips}$) compared with contralateral stimulation ($DA_{con}$) at identical depths. $n = 10$ animals per group. Data are average ± SEM. (*B* and *D*) Representative dopamine response in the contralateral NAc (*B*) and DMS (*D*) to optogenetic (blue) and electrical (red) stimulation of VTA or SN.

this equal release was unique to the DMS (Fig. S2). In addition, contralateral release was not due to electrical spread to the ipsilateral hemisphere, given that lidocaine infusions in the ipsilateral SN/VTA did not affect the release evoked by contralateral stimulation (Fig. S3).

We confirmed the origin of contralateral release using optogenetics to activate only dopaminergic neurons. We drove channelrhodopsin-2 (ChR2) expression in dopamine neurons using a tyrosine hydroxylase (TH) promoter (37, 38). Light stimulation of the VTA elicited dopamine release in the contralateral NAc roughly equivalent to electrical stimulation (Fig. 3*B*). A similar release was seen in the DMS following stimulations of the contralateral SN (Fig. 3*D*). We found ChR2 expression in the contralateral DMS in the absence of viral spread between hemispheres in the SN (Figs. S4 and S5) and VTA (Fig. S6).

**Contralateral Dopamine Release Is Differentially Regulated.** To investigate the differences in dopamine release from contralateral and ipsilateral projections, we administered D2 antagonist raclopride (RAC; 2 mg/kg i.p.) and dopamine transporter inhibitor GBR-12909 (GBR; 15 mg/kg i.p.) and measured their effects on evoked dopamine. There were no differences in D2-like regulation between the contralateral and ipsilateral projections to the DMS (Fig. 4*A*). In contrast, D2 autoreceptors in the NAc exerted more control over dopamine release from contralateral compared with ipsilateral projections, evidenced by a much greater RAC response on the contralateral side (525 ± 135.3% vs. 204 ± 26.5%, respectively; $n = 7$; $F_{(3,22)} = 4.9$, $P < 0.05$) (Fig. 4*B*). Thus, enhanced regulation by D2 might account for the discrepancy in dopamine concentrations evoked in the ipsilateral and contralateral NAc. We also found an increased response to GBR in the DMS following contralateral SN stimulation relative to ipsilateral stimulation (1260 ± 301% vs. 694 ± 199%, respectively; $n = 7$; $F_{(3,26)} = 5.7$, $P < 0.05$), but not in the NAc (Fig. 4 *A* and *B*). To exclude the effects of supraphysiological stimulation frequency on dopamine release, we delivered 10-Hz stimulations to the contralateral VTA and SN, resulting in small, yet physiologically relevant concentrations (Fig. S7).

**Contralateral Release Is Not Solely Compensatory.** Parkinson's disease is often modeled with unilateral 6-OHDA lesions. Although small dopamine concentrations remain in lesioned animals (39), the extent to which contralateral projections compensate for depletion is unknown. Given that the DMS exhibited hemispherically equivalent release, we chose it as a site for monitoring changes in contralateral dopamine release after depletion. We used unilateral 6-OHDA lesions of the SN and recorded dopamine release in the lesioned hemisphere. At 2 wk after treatment, we validated the lesions by measuring ipsilaterally biased rotations after administration of 2.5 mg/kg AMPH (effect of 6-OHDA treatment, $F_{(1,12)} = 38.32$; effect of AMPH administration, $F_{(1,12)} = 49.55$, $P < 0.001$, two-way repeated-measures ANOVA) (Fig. 5*B*; TH immunoreactivity in Fig. S8). After 3 d, animals were anesthetized, and dopamine was measured in the DMS ipsilateral to the lesion. Stimulations were delivered to ipsilateral (lesioned) and contralateral SN (Fig. 5 *A* and *C*). Ipsilateral dopamine efflux was ablated following lesioned SN stimulation relative to controls (0.03 ± 0.007 μM vs. 0.15 ± 0.024 μM; $n = 7$; $F_{(3,24)} = 8.3$, $P < 0.001$) (Fig. 5*D*). Stimulation of the contralateral/untreated SN resulted in dopamine release in the same recording location (Fig. 5*D*). Surprisingly, the lesioned and control animals showed no differences in dopamine release following contralateral SN stimulation, suggesting that contralateral projections in 6-OHDA–treated rats do not compensate via increased release (0.10 ± 0.01 μM vs. 0.12 ± 0.02 μM; $n = 7$; $P > 0.05$) (Fig. 5*D*).

Dopamine denervation drives homeostatic changes in striatal signaling (40), such as increased D2 expression in indirect pathway neurons (29). To test for D2-like adaptations in intact contralateral projections after unilateral dopamine depletion, we measured the effect of D2 antagonist RAC (2 mg/kg i.p.) on release in the lesioned DMS. RAC produced a larger increase in contralaterally evoked dopamine in lesioned animals compared with control animals (674 ± 98.3% vs. 401 ± 79.9%; $n = 7$; $t_{(13)}$=2.2, $P < 0.05$), confirming adaptation after dopamine depletion.

Finally, we measured spontaneous dopamine efflux in awake animals at 2 wk after unilateral 6-OHDA treatment. We found spontaneous dopamine transients in the DMS of sham-lesioned animals that increased following AMPH administration (Fig. 5*E*), in agreement with previous studies (31). In the 6-OHDA–lesioned animals, spontaneous dopamine transients in the DMS ipsilateral to the SN lesion were not present under vehicle administration, but were elicited by AMPH administration (Fig. 5*F*). Thus, AMPH-induced dopamine release appears to arise from intact contralateral projections in unilaterally lesioned animals.

## Discussion

Our findings reveal previously undescribed interhemispheric communication in the mesencephalic dopamine system of rats. First, we found that optogenetic and electrical stimulation of dopamine cells elicited physiologically relevant release in the contralateral striatum. Compared with ipsilateral projections, contralateral

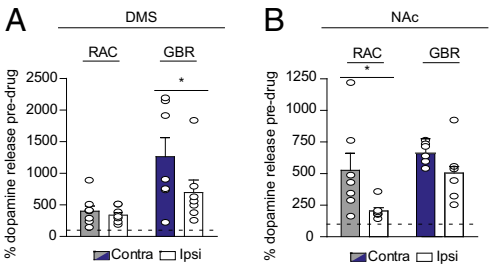


**Fig. 4.** Contralateral dopamine release is differentially regulated in the DMS (*A*) and the NAc (*B*). The graphs show the average increase in contralaterally (gray/blue) or ipsilaterally (white) evoked dopamine after RAC and GBR administration as a percentage of baseline value. $n = 6$–8 animals per group. Data are average ± SEM with individual experiments overlaid. *$P < 0.05$, ANOVA with Bonferroni post hoc correction.

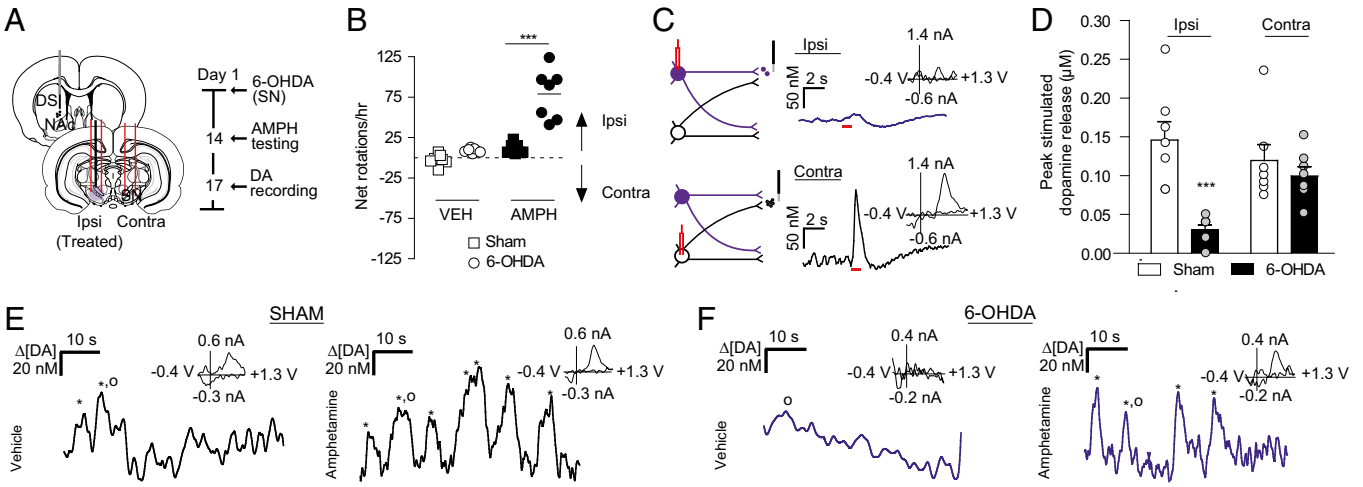


**Fig. 5.** Activation of the contralateral SN evokes dopamine release in 6-OHDA–lesioned rats. (*A*) Schematic of 6-OHDA delivery through a cannulated stimulating electrode, recording locations in the ipsilateral DMS, and contralateral stimulating electrode placement. (*B*) Rotational behavior in sham-treated and 6-OHDA–lesioned rats treated with saline vehicle (VEH), followed by 2.5 mg/kg AMPH. ***$P < 0.001$, repeated-measures two-way ANOVA with Bonferroni post hoc correction. (*C*) Representative dopamine release in the DMS following stimulation (red bar) of 6-OHDA–treated SNs (purple) and contralateral SNs (black). Cyclic voltammograms are shown as well. (*D*) Average ± SEM maximal dopamine concentrations evoked from stimulating 6-OHDA–treated and contralateral SNs in lesioned and sham-treated rats. $n = 7$ per group. ***$P < 0.001$, ANOVA with Bonferroni post hoc test. (*E* and *F*) Representative dopamine transients (asterisks) in the DMS in awake sham-treated (*E*, black), or 6-OHDA–treated (*F*, purple) rats following saline (VEH) and AMPH administration. Cyclic voltammograms corresponding to the dopamine transients, denoted by the circles, are shown as well.

projections from the VTA released less dopamine in the NAc and were more tightly controlled by D2 autoreceptors. In contrast, dopamine release in the DMS was equivalent following contralateral or ipsilateral SN stimulation and accompanied similar D2 control in both hemispheres. Second, we found that ∼75% of spontaneous NAc dopamine transients synchronized between hemispheres in freely moving rats, which increased to 100% following AMPH administration. Finally, we showed that contralateral projections from SN neurons were functional in the hemiparkinsonian state, but did not compensate by increased dopamine release. Instead, D2 control on contralateral projections was increased after unilateral 6-OHDA treatment. Contralateral SN projections can be stimulated with amphetamine to evoke dopamine transients in the lesioned striatum of awake animals. These results establish for the first time, to our knowledge, that transient dopamine concentrations are synchronous between hemispheres, and that the dopamine system has functional contralateral projections, with implications for interhemispheric adaptations in Parkinson's disease. Furthermore, our data indicate that psychostimulants, such as AMPH, play a role in coupling dopamine transients between hemispheres.

Anatomic studies have described ∼5% of midbrain dopamine neurons as projecting contralaterally to their origin (22, 23). In agreement with this, we found lower dopamine concentrations in the NAc after contralateral VTA stimulation compared with after ipsilateral VTA stimulation (Fig. 3*A*). Interestingly, dopamine release from contralateral VTA neurons was more regulated by D2 autoreceptors. Dopamine released from ipsilateral projections may occupy D2 receptors on terminals from the contralateral hemisphere, attenuating release from contralateral VTA. Under intense stimulation, or with disruption of regulation mechanisms, dopamine can be released from these fibers. Consistent with this idea, dopamine receptor antagonism in the contralateral NAc has been found to suppress intra-VTA self-stimulation in the ipsilateral hemisphere (24), corroborating cross-hemispheric functionality and providing behavioral significance.

Surprisingly, when we placed our recording electrode in the DMS and stimulated contralateral or ipsilateral SN, we found similar release amplitudes regardless of the stimulated hemisphere (Fig. 3*C*). This property was unique to the DMS, as the evoked dopamine ratio in the dorsolateral striatum was more similar to that in the NAc (Fig. S2). Similar D2 regulation in both hemispheres accompanied hemispherically equivalent release in the contralateral DMS, in contrast to D2 regulation of contralateral/ipsilateral VTA projections. Based on the confirmation of our findings using optogenetics, contralateral dopamine release is driven by dopamine neurons; however, optical activation does not preclude the effects of glutamate corelease (41), which may facilitate hemispherically equivalent release.

Dopamine transients are increased following administration of drugs of abuse (12), and this appears to mediate their reinforcing properties (14). Dopamine transients have been studied extensively (1–13, 31–35); however, previous measurements were restricted to a single hemisphere, including those using a magnetic resonance imaging-compatible dopamine reporter (42), and few microdialysis experiments performed bilateral measurements (43). In the present work, we measured spontaneous dopamine efflux with millisecond time resolution in both hemispheres simultaneously and found synchronicity in release. In agreement with previous reports (11), synchronized dopamine concentrations exhibited variability on a subminute timescale (Fig. 1*D*), but on average, transient concentrations over 30 min were comparable between the hemispheres (Fig. 1*E*). The apparent bilateral synchrony in NAc dopamine release shows that although transients are heterogeneous within subregions (11), their occurrence is coupled between the hemispheres.

Interestingly, after AMPH administration, all dopamine efflux became synchronized between the hemispheres. Because NAc dopamine transients originate from VTA cell firing (8, 9), and amphetamine-induced dopamine release occurs in an action potential-dependent manner (44), coupled dopamine transients reflect synchronicity within the VTA that could arise from several mechanisms. During psychostimulant-induced excitation, VTA cells display slow, rhythmic oscillations (45). These oscillations allow neurons to become more sensitive to the precise timing of synaptic inputs and aid in synchronizing patterns of neuronal activity (46). Thus, amphetamine may synchronize firing in the VTA between hemispheres, or synchronize contralaterally and ipsilaterally projecting neurons within a hemisphere. Synchronicity in dopamine transients may result from neurotensin release in the VTA. Intra-VTA neurotensin activates dopamine neurons and contributes to behavioral sensitization after administration of psychostimulants (47). The parabrachial nucleus is one source of

neurotensinergic projections to the VTA (48) and projects bilaterally to midbrain dopamine neurons (49).

Regardless of the mechanism, the synchronicity in dopamine release between hemispheres uncovered here establishes that chemical signaling, like physiological activity (50), is tightly coupled across the brain. Given that amphetamine-induced dopamine transients remained in the unilaterally lesioned animals, it is apparent that interhemispherical connectivity contributes to psychostimulant-induced dopamine fluctuations. Dopamine transients, which have been shown to be important in drug abuse (14), clearly arise from bilateral interactions. Furthermore, amphetamines are used to treat attention deficit hyperactivity disorder (ADHD), and patients with ADHD have abnormal frontostriatal asymmetry (51). The observed synchronicity in dopamine signaling after amphetamine administration may contribute to its therapeutic effects in individuals with ADHD. Although further research is needed to establish the mechanisms that coordinate dopamine transient coupling, the present study establishes that dopamine fluctuations display synchrony between hemispheres.

Contralateral projections may balance dopamine concentrations between hemispheres after dopamine depletion. However, when the SN was 6-OHDA lesioned, we found dopamine release from the contralateral, unlesioned SN was equivalent in lesioned and control animals. This finding was surprising, because these projections are thought to compensate for depletion via increased release (30). Instead, we found enhanced D2 control over release in the lesioned hemisphere, supporting the previous finding of increased D2 expression after dopamine depletion (29).

When we extended our measurements to awake animals, we found spontaneous transients in the DMS of sham-lesioned animals that were not present in the 6-OHDA–lesioned animals. Dopamine transients were elicited in the lesioned hemisphere with AMPH, however. Considering that D2 receptors exerted more control over contralateral dopamine release in lesioned animals, and that amphetamine attenuates D2 function (52), we believe that this release arose from the intact contralateral projections. With the perturbation introduced by amphetamine, contralateral projections may release dopamine into the depleted hemisphere. Indeed, dopamine cell firing between hemispheres has been seen to normalize after the activation of dopamine receptors in 6-OHDA–lesioned animals (53). Previous work in primates (54) and rats (55) has alluded to interhemispheric adaptations following nigrostriatal damage. The data presented here establish a functional role for interhemispheric dopamine projections after unilateral 6-OHDA treatment.

In summary, this work demonstrates the functional significance of interhemispheric communication in dopaminergic signaling. Activation of midbrain dopamine neurons evokes physiologically relevant dopamine release in the contralateral striatum of rats that synchronizes between the hemispheres. D2 autoreceptors from contralateral VTA projections exert more control over NAc dopamine release relative to the ipsilateral projections, in contrast to DMS release via SN stimulation. Selective activation confirmed that dopaminergic neurons drive contralateral release. Furthermore, we found that contralateral release was not solely compensatory, because similar amounts of dopamine were evoked after contralateral SN stimulation in 6-OHDA–treated and control rats. These data are the first to demonstrate the functional nature of cross-hemispheric dopamine projections, and provide a new context for the plasticity of striatal synapses after unilateral manipulation. Crossing projections likely facilitate the observed coupling of dopamine transients. Moreover, our findings provide additional insight into recently reported receptor alterations (25–29), showing that the lesioned hemisphere is not completely dopamine-deprived. Low concentrations released from contralateral projections, such as those reported here after AMPH administration, likely influence receptor sensitivity in the lesioned hemisphere, and should be accounted for in future studies. The previously unappreciated cross-hemispheric functionality revealed here also may be useful in devising new therapies for dysregulated dopamine signaling.

## Methods

Additional details are provided in *SI Methods*.

**Animal Care.** All experiments were performed in accordance with guidelines of the Institutional Animal Care and Use Committees at the University of North Carolina at Chapel Hill and Wake Forest University. Sprague–Dawley rats (males, 270–400 g; Charles River Laboratories) were given food and water ad libitum and pair-housed in University of North Carolina or Wake Forest University animal facilities under a 12-h:12-h light:dark cycle. All experiments were performed during the 12-h light period. To reduce the number of animals and minimize their suffering, we limited the awake measurements to three per treatment group, sufficient to demonstrate the effect in each animal. For anesthetized experiments, we selected 5–10 animals, typical of voltammetric studies. In total, 3 animals were used for bilateral transient measurements, 20 were used for 6-OHDA studies, 53 were used for mapping/pharmacology, and 10 were used for optogenetic experiments.

**Spontaneous Dopamine Measurements.** Rats underwent stereotaxic surgery under isofluorane anesthesia. In brief, two guide cannulas (BASi) were implanted bilaterally in the NAc [anteroposterior (AP), +1.3; mediolateral (ML), ± 2.1 mm, ±10° to the perpendicular], a bipolar stimulating electrode (Plastics One) in the right VTA (AP, −5.2; ML, +1.0; DV, 8.5 mm), and a third cannula in the left hemisphere for an Ag/AgCl reference. After 3 d of recovery, carbon fiber microelectrodes were lowered bilaterally into the NAc of the awake animals through microdrives. Voltammetric measurements of dopamine transients were performed as described previously (7, 38) using High-Definition Cyclic Voltammetry software. A triangular scan (−0.4 to +1.3V, 400 V/s) was applied to the working electrode every 100 ms to detect changes in dopamine concentration. Spontaneous dopamine efflux was measured for 30 min after administration of vehicle (VEH) (saline, 1 mL/kg i.p.), and 30 min after administration of AMPH (2.5 mg/kg i.p.; Sigma-Aldrich). Animals were then anesthetized (urethane, 1.5 g/kg), after which VTA stimulation was delivered to construct voltammograms for principal component analysis using an in vitro calibration factor (10 nA/μM) (56). Only transients exceeding three times the SD of the noise in dopamine traces obtained by principal component regression were considered spontaneous dopamine.

**6-OHDA Lesions.** Here 3 μL of 10 mM 6-OHDA HBr/0.01% wt/vol ascorbic acid (Sigma-Aldrich) in saline (0.9%) or saline (sham) was infused into the right SN (AP, −5.8 mm; ML, +2.0 mm; DV, −7.8 mm) through a cannulated stimulating electrode (Plastics One) at 1 μL/min. After being allowed to recover from the 6-OHDA lesions for 2 wk, rats were placed in a clear plastic bowl (30 cm diameter, 20 cm high) and videotaped for spontaneous rotational behavior after administration of 2.5 mg/kg AMPH. At 3 d after scoring of rotations, rats were anesthetized (urethane, 1.5 g/kg), and a second stimulating electrode was placed in the left SN (AP, −5.8; ML, −2.0; DV, −7.8 mm). A carbon fiber electrode was lowered into the right DMS (AP, +1.2; ML, +2.0; DV, −4.0 to −6.2 mm) in 200-μm intervals. An Ag/AgCl reference electrode was placed contralateral to the working electrode. Dopamine release was evoked using 1-s, 300-μA stimulation pulses applied at 60 Hz using two constant current isolators (NL800; NeuroLog) and compared between hemispheres. In a subset of freely moving animals, a carbon fiber electrode was lowered into the DMS (DV, 6.0 mm). Spontaneous dopamine transients were recorded after VEH (1 mL/kg saline) and AMPH (2.5 mg/kg) administration. Animals were then anesthetized (urethane, 1.5 mg/kg), and electrical stimulation was delivered to treated and contralateral SNs to confirm lesion efficacy.

**Mapping of Contralateral Dopamine Release.** Naive rats were anesthetized with urethane, and holes were drilled for recording electrodes in the NAc or DMS (NAc: AP, +1.3 mm; ML, +1.3 mm; DMS: as above) and a stimulating electrode in the VTA or SN (VTA: AP, −5.2; ML, ±1.0 mm; SN: AP, −5.8 mm; ML, ±2.0 mm). The stimulating electrode was held at a constant depth contralateral to the carbon fiber electrode (VTA: −8.4 mm DV, SN: −7.8 mm DV) while the carbon fiber electrode was lowered in 200-μm increments. Then 300-μA electrical stimulation (60 Hz, 1 s) was applied with NeuroLogs (NL800). Once maximal dopamine release was attained at the working electrode, the stimulating electrode was adjusted ventrally in 200-μm intervals to map the effect of stimulation location on release. The stimulating electrode was removed from the contralateral hemisphere and lowered ventrally through the ipsilateral hemisphere. In a subset of animals (five DMS, five NAc), 10-Hz stimulations were delivered to the contralateral SN/VTA. We also examined dopamine release in the dorsolateral striatum (AP, +0.5 mm; ML, +3.5 mm; $n = 5$), and as evoked by PPTg stimulation (AP, −7.8; ML, ±2.0 mm; $n = 5$).

**Pharmacology.** Baseline release was recorded for 20 min by repeating the 1-s electrical stimulation every 2 min. Release was monitored for 30 min after D2 receptor antagonism [s-(−)-RAC HCl, 2 mg/kg i.p.; Sigma-Aldrich], and for

30 min after subsequent dopamine transporter inhibition (GBR-12909, 15 mg/kg i.p.; Sigma-Aldrich).

**Statistics.** Statistical analyses were performed using GraphPad Prism, and no data were removed. One-way ANOVA with Bonferroni post hoc correction was used to determine significant differences between groups. Two-way repeated-measures ANOVA was applied to determine significant increases in dopamine transients and ipsilateral rotations after AMPH administration. A two-tailed unpaired *t* test was used to determine differences in RAC response between 6-OHDA–lesioned and sham-lesioned animals.

**ACKNOWLEDGMENTS.** We thank Michael Bruno for immunohistochemistry assistance and Elyse Dankoski for comments on the manuscript. This work was funded by the National Institutes of Health (Grants DA10900, to R.M.W., and AA022449, to E.A.B.) and the Russian Science Foundation (Grant 4-50-00069, to R.R.G.).

1. Wassum KM, Ostlund SB, Maidment NT (2012) Phasic mesolimbic dopamine signaling precedes and predicts performance of a self-initiated action sequence task. *Biol Psychiatry* 71(10):846–854.
2. Sugam JA, Day JJ, Wightman RM, Carelli RM (2012) Phasic nucleus accumbens dopamine encodes risk-based decision-making behavior. *Biol Psychiatry* 71(3):199–205.
3. Phillips PE, Stuber GD, Heien ML, Wightman RM, Carelli RM (2003) Subsecond dopamine release promotes cocaine seeking. *Nature* 422(6932):614–618.
4. Day JJ, Roitman MF, Wightman RM, Carelli RM (2007) Associative learning mediates dynamic shifts in dopamine signaling in the nucleus accumbens. *Nat Neurosci* 10(8): 1020–1028.
5. Owesson-White CA, Cheer JF, Beyene M, Carelli RM, Wightman RM (2008) Dynamic changes in accumbens dopamine correlate with learning during intracranial self-stimulation. *Proc Natl Acad Sci USA* 105(33):11957–11962.
6. Roitman MF, Stuber GD, Phillips PE, Wightman RM, Carelli RM (2004) Dopamine operates as a subsecond modulator of food seeking. *J Neurosci* 24(6):1265–1271.
7. Saddoris MP, Cacciapaglia F, Wightman RM, Carelli RM (2015) Differential dopamine release dynamics in the nucleus accumbens core and shell reveal complementary signals for error prediction and incentive motivation. *J Neurosci* 35(33): 11572–11582.
8. Sombers LA, Beyene M, Carelli RM, Wightman RM (2009) Synaptic overflow of dopamine in the nucleus accumbens arises from neuronal activity in the ventral tegmental area. *J Neurosci* 29(6):1735–1742.
9. Cacciapaglia F, Wightman RM, Carelli RM (2011) Rapid dopamine signaling differentially modulates distinct microcircuits within the nucleus accumbens during sucrose-directed behavior. *J Neurosci* 31(39):13860–13869.
10. Robinson DL, Heien ML, Wightman RM (2002) Frequency of dopamine concentration transients increases in dorsal and ventral striatum of male rats during introduction of conspecifics. *J Neurosci* 22(23):10477–10486.
11. Wightman RM, et al. (2007) Dopamine release is heterogeneous within microenvironments of the rat nucleus accumbens. *Eur J Neurosci* 26(7):2046–2054.
12. Cheer JF, et al. (2007) Phasic dopamine release evoked by abused substances requires cannabinoid receptor activation. *J Neurosci* 27(4):791–795.
13. Stuber GD, Wightman RM, Carelli RM (2005) Extinction of cocaine self-administration reveals functionally and temporally distinct dopaminergic signals in the nucleus accumbens. *Neuron* 46(4):661–669.
14. Covey DP, Roitman MF, Garris PA (2014) Illicit dopamine transients: Reconciling actions of abused drugs. *Trends Neurosci* 37(4):200–210.
15. Schultz W (2015) Neuronal reward and decision signals: From theories to data. *Physiol Rev* 95(3):853–951.
16. Berridge KC, Robinson TE (1998) What is the role of dopamine in reward: Hedonic impact, reward learning, or incentive salience? *Brain Res Brain Res Rev* 28(3):309–369.
17. Crocker AD (1997) The regulation of motor control: An evaluation of the role of dopamine receptors in the substantia nigra. *Rev Neurosci* 8(1):55–76.
18. Baik JH, et al. (1995) Parkinsonian-like locomotor impairment in mice lacking dopamine D2 receptors. *Nature* 377(6548):424–428.
19. Costa RM, et al. (2006) Rapid alterations in corticostriatal ensemble coordination during acute dopamine-dependent motor dysfunction. *Neuron* 52(2):359–369.
20. Andén N-E, Fuxe K, Larsson K, Olson L, Ungerstedt U (1966) Ascending monoamine neurons to the telencephalon and diencephalon. *Acta Physiol Scand* 67(3-4):313–326.
21. Nauta WJ, Smith GP, Faull RL, Domesick VB (1978) Efferent connections and nigral afferents of the nucleus accumbens septi in the rat. *Neuroscience* 3(4-5):385–401.
22. Jaeger CB, Joh TH, Reis DJ (1983) The effect of forebrain lesions in the neonatal rat: Survival of midbrain dopaminergic neurons and the crossed nigrostriatal projection. *J Comp Neurol* 218(1):74–90.
23. Geisler S, Zahm DS (2005) Afferents of the ventral tegmental area in the rat-anatomical substratum for integrative functions. *J Comp Neurol* 490(3):270–294.
24. Steinberg EE, et al. (2014) Positive reinforcement mediated by midbrain dopamine neurons requires D1 and D2 receptor activation in the nucleus accumbens. *PLoS One* 9(4):e94771.
25. Fieblinger T, et al. (2014) Mechanisms of dopamine D1 receptor-mediated ERK1/2 activation in the parkinsonian striatum and their modulation by metabotropic glutamate receptor type 5. *J Neurosci* 34(13):4728–4740.
26. Capper-Loup C, Kaelin-Lang A (2013) Locomotor velocity and striatal adaptive gene expression changes of the direct and indirect pathways in parkinsonian rats. *J Parkinsons Dis* 3(3):341–349.
27. Thiele SL, et al. (2014) Selective loss of bi-directional synaptic plasticity in the direct and indirect striatal output pathways accompanies generation of parkinsonism and l-DOPA–induced dyskinesia in mouse models. *Neurobiol Dis* 71:334–344.
28. Day M, et al. (2006) Selective elimination of glutamatergic synapses on striatopallidal neurons in Parkinson disease models. *Nat Neurosci* 9(2):251–259.
29. Gerfen CR (2000) Molecular effects of dopamine on striatal-projection pathways. *Trends Neurosci* 23(10, Suppl):S64–S70.
30. Nieoullon A, Cheramy A, Glowinski J (1977) Interdependence of the nigrostriatal dopaminergic systems on the two sides of the brain in the cat. *Science* 198(4315):416–418.
31. Daberkow DP, et al. (2013) Amphetamine paradoxically augments exocytotic dopamine release and phasic dopamine signals. *J Neurosci* 33(2):452–463.
32. Hamid AA, et al. (2016) Mesolimbic dopamine signals the value of work. *Nat Neurosci* 19(1):117–126.
33. Howe MW, Tierney PL, Sandberg SG, Phillips PE, Graybiel AM (2013) Prolonged dopamine signalling in striatum signals proximity and value of distant rewards. *Nature* 500(7464):575–579.
34. Syed EC, et al. (2016) Action initiation shapes mesolimbic dopamine encoding of future rewards. *Nat Neurosci* 19(1):34–36.
35. Wheeler DS, et al. (2015) Drug predictive cues activate aversion-sensitive striatal neurons that encode drug seeking. *J Neurosci* 35(18):7215–7225.
36. Park J, Takmakov P, Wightman RM (2011) In vivo comparison of norepinephrine and dopamine release in rat brain by simultaneous measurements with fast-scan cyclic voltammetry. *J Neurochem* 119(5):932–944.
37. Gompf HS, Budygin EA, Fuller PM, Bass CE (2015) Targeted genetic manipulations of neuronal subtypes using promoter-specific combinatorial AAVs in wild-type animals. *Front Behav Neurosci* 9:152.
38. Bass CE, et al. (2013) Optogenetic stimulation of VTA dopamine neurons reveals that tonic, but not phasic, patterns of dopamine transmission reduce ethanol self-administration. *Front Behav Neurosci* 7:173.
39. Zigmond MJ, Hastings TG, Abercrombie ED (1992) Neurochemical responses to 6-hydroxydopamine and L-dopa therapy: Implications for Parkinson's disease. *Ann N Y Acad Sci* 648:71–86.
40. Zigmond MJ, Abercrombie ED, Berger TW, Grace AA, Stricker EM (1990) Compensations after lesions of central dopaminergic neurons: Some clinical and basic implications. *Trends Neurosci* 13(7):290–296.
41. Zhang S, et al. (2015) Dopaminergic and glutamatergic microdomains in a subset of rodent mesoaccumbens axons. *Nat Neurosci* 18(3):386–392.
42. Lee T, Cai LX, Lelyveld VS, Hai A, Jasanoff A (2014) Molecular-level functional magnetic resonance imaging of dopaminergic signaling. *Science* 344(6183):533–535.
43. Buck K, Ferger B (2008) Intrastriatal inhibition of aromatic amino acid decarboxylase prevents l-DOPA–induced dyskinesia: A bilateral reverse in vivo microdialysis study in 6-hydroxydopamine lesioned rats. *Neurobiol Dis* 29(2):210–220.
44. Covey DP, Bunner KD, Schuweiler DR, Cheer JF, Garris PA (2016) Amphetamine elevates nucleus accumbens dopamine via an action potential-dependent mechanism that is modulated by endocannabinoids. *Eur J Neurosci*, 10.1111/ejn.13248.
45. Shi W-X, Pun C-L, Zhou Y (2004) Psychostimulants induce low-frequency oscillations in the firing activity of dopamine neurons. *Neuropsychopharmacology* 29(12):2160–2167.
46. Volgushev M, Chistiakova M, Singer W (1998) Modification of discharge patterns of neocortical neurons by induced oscillations of the membrane potential. *Neuroscience* 83(1):15–25.
47. Panayi F, et al. (2005) Endogenous neurotensin in the ventral tegmental area contributes to amphetamine behavioral sensitization. *Neuropsychopharmacology* 30(5): 871–879.
48. Geisler S, Zahm DS (2006) Neurotensin afferents of the ventral tegmental area in the rat: [1] re-examination of their origins and [2] responses to acute psychostimulant and antipsychotic drug administration. *Eur J Neurosci* 24(1):116–134.
49. Watabe-Uchida M, Zhu L, Ogawa SK, Vamanrao A, Uchida N (2012) Whole-brain mapping of direct inputs to midbrain dopamine neurons. *Neuron* 74(5):858–873.
50. Shen K, et al. (2015) Stable long-range interhemispheric coordination is supported by direct anatomical projections. *Proc Natl Acad Sci USA* 112(20):6473–6478.
51. Silk TJ, et al. (2015) Abnormal asymmetry in frontostriatal white matter in children with attention deficit hyperactivity disorder. *Brain Imaging Behav*, 10.1007/s11682-015-9470-9.
52. Calipari ES, et al. (2014) Amphetamine self-administration attenuates dopamine D2 autoreceptor function. *Neuropsychopharmacology* 39(8):1833–1842.
53. Chen MT, Morales M, Woodward DJ, Hoffer BJ, Janak PH (2001) In vivo extracellular recording of striatal neurons in the awake rat following unilateral 6-hydroxydopamine lesions. *Exp Neurol* 171(1):72–83.
54. Salvatore MF, Gerhardt GA, Dayton RD, Klein RL, Stanford JA (2009) Bilateral effects of unilateral GDNF administration on dopamine- and GABA-regulating proteins in the rat nigrostriatal system. *Exp Neurol* 219(1):197–207.
55. Yang J, Sadler TR, Givrad TK, Maarek JM, Holschneider DP (2007) Changes in brain functional activation during resting and locomotor states after unilateral nigrostriatal damage in rats. *Neuroimage* 36(3):755–773.
56. Rodeberg NT, et al. (2015) Construction of training sets for valid calibration of in vivo cyclic voltammetric data by principal component analysis. *Anal Chem* 87(22): 11484–11491.